UNIVERSITY OF TARTU
Faculty of Science and Technology
Institute of Physics

Sander Suurpere

MULTIPLE SCATTERING SIMULATIONS FOR DETECTION APPLICATIONS

Bachelor's thesis (12 ECTS)

Supervisors:
Volodymyr Gulik, PhD
Madis Kiisk, PhD

Tartu 2017

Multiple scattering simulations for detection applications

Abstract

The physical phenomenon in which a charged particle changes its direction of motion in the proximity of an atomic nucleus is called Rutherford scattering. When a charged particle passes through matter, it experiences several sequential scatterings and as a result it exits the material in a random angle. This process is referred to as multiple scattering.

Multiple scattering is an important aspect in the design of certain radiographic and tomographic devices which exploit secondary cosmic rays. Implementing a naturally occurring particle flux in the design of a detection system is a good way to prevent the occurrence of additional doses of ionizing radiation and to reduce the number of additional particle sources associated with traditional radiography methods.

The scientific literature engaged in studying detection methods based on the multiple scattering of cosmic ray muons has been largely concerned with the detection of high-Z (atomic number) materials inside a low-Z environment. It is unclear whether it is possible to construct a device for detecting low-Z materials inside a similar-Z environment by using cosmic rays alone and exactly to what extent would this device exploit the process of multiple scattering.

The aim of this thesis is to compare the multiple scattering of muons in different (mostly low-Z) materials and estimate the limits of applicability of this method of detection. The main tool used in this thesis is a Monte Carlo software package called Geant4. The work comprised of developing the necessary software, running the simulations with objects consisting of various materials and analyzing the data. The results show that a detection device implementing the multiple scattering of cosmic ray muons alone is not a realistic way to detect low-Z objects hidden inside a low-Z environment.

Keywords: Geant4, Monte Carlo methods, multiple scattering, muon
Physical Sciences P211 High energy interactions, cosmic rays

Mitmikhajumise modelleerimine tuvastussüsteemide rakendusteks
Lühikokkuvõte

Rutherfordi hajumiseks nimetatakse füüsikalist nähtust, mille käigus muudab ainesse sisenenud laetud osake elektromagnetilise vastastikmõju tõttu aine koostisesse kuuluvate tuumade läheduses oma liikumissuunda. Mitme järjestikuse Rutherfordi hajumise tagajärjel väljub laetud osake ainest juhusliku nurga all ning seda protsessi nimetatakse mitmikhajumiseks.

Mitmikhajumise nähtus on olulisel kohal teatud radiograafia- ja tomograafiaseadmete ehituses, mis põhinevad kosmilisel sekundaarkiirgusel. Looduses pidevalt esineva ning paratamatu osakestevoo rakendamine tuvastussüsteemide töös võimaldab vältida traditsioonilistele radiograafiameetoditele (röngtenkiirgus) omaseid lisakiirgudoose ning tehislikke kiirgusallikaid.

Müüonite mitmikahjumise tuvastussüsteeme uuriv teaduskirjandus põhineb peamiselt kõrge Z-ga (laenguarvuga) materjalide identifitseerimisel madala Z-ga keskkonnas. On selgusetu, kas ja mil määral on kosmilise kiirgusega võimalik tuvastada madala Z-ga aineid sarnase Z-ga keskkonnas ning kui suurt rolli mängiks sellises seadmes mitmikhajumine. Samuti pole hetkel võimalik öelda, milline oleks täpselt sellise tuvastusseadme tehniline teostus.

Käesoleva töö eesmärgiks on võrrelda mitmikhajumist erinevates, enamasti madala Z-ga ainetes ning hinnata seeläbi meetodi rakendatavuse piire. Peamise töövahendina kasutati Monte Carlo meetoditel põhinevat tarkvarapaketti Geant4. Praktiline osa koosnes tarkvara koostamisest, koodi jooksutamisest erinevate materjalidega ning andmete töötlemisest. Töö tulemused kinnitavad, et ainuüksi mitmikahjumisel põhinevad radiograafiaseadmed ei ole optimaalsed vahendid madala Z-ga ainete tuvastamiseks keskkondades, mis koosnevad samuti madala Z-ga ainetest.

Märksõnad: Geant4, Monte Carlo meetodid, mitmikhajumine, müüon
Reaalteadused P211 Kõrgenergeetiliste vastasmõjude uuringud, kosmiline kiirgus

Contents

Abbreviations

CLHEP – A Class Library for High Energy Physics
HEU – Highly Enriched Uranium
RMS – Root Mean Square
RPM – Radiation Portal Monitor
SNM – Special Nuclear Material
WGP – Weapons-Grade Plutonium

Introduction

The motivation behind studying various screening methods stems from the need to ensure national security by reducing the illicit traffic of specific materials in border crossings, airports and other critical points. Monitoring the flow of goods and people creates the necessity to reduce radiation hazards related to some conventional detection methods and to speed up the process.

Currently, various methods exist for the detection of SNM (e.g. highly enriched uranium or weapons-grade plutonium). The so called passive methods of detection do not use any external source of radiation to detect a SNM. Instead, passive methods rely on any intrinsic radiation that is emitted from the SNM. This includes characteristic photon lines as well as neutrons from spontaneous fission. Alternatively, an active method of detection is any method that uses an external source of radiation to induce reactions with potential hidden materials. In order to prevent the use of any added radiation sources, a detector exploiting natural background radiation, e.g. cosmic ray muons or electrons, can be used instead. The question arises, whether this type of detector would in some way be capable of discovering any low-Z illicit materials (explosives, drugs) as well.

A good way to determine whether some physical system has any chance of producing expected results is to create a computational model of that system. A software platform called Geant4 is the main tool used in the simulations related to this thesis. Geant4 is an open source toolkit developed in CERN that implements Monte Carlo methods and is specifically designed for particle simulations. Geant4 is capable of modeling a wide variety of elementary particles and physical processes to which these particles are sensitive to, including multiple scattering.

The aim of this thesis is to simulate the behavior of cosmic ray muons in different types of (mostly) low-Z materials with emphasis on finding the average deflection angles of the particles. The thesis is divided into four chapters. The first chapter is dedicated to giving an overview of the background knowledge needed to understand the simulation. The second chapter describes the methodology used in the computations, namely Monte Carlo methods and the Geant4 toolkit. The third and fourth chapters describe the simulation setup and results.

Chapter 1

Background

One of the hindrances of conventional radiography is the fact that highly penetrating gamma rays are responsible for large radiation doses. On the other hand, less harmful incident doses have no ability to penetrate dense materials. This has led to the development of alternative detection methods such as muon radiography and tomography [1, 2, 3, 4, 5, 6].

1.1 Cosmic ray muons

Cosmic rays are generally divided into primary and secondary flux. Primary flux consists of particles which are accelerated at astrophysical sources [7]. The intensity of primary nucleons incident at the top of the terrestrial atmosphere can be approximated by

$$I_N(E) \approx 1.8 \cdot 10^4 \left(\frac{E}{1\text{GeV}} \right)^{-\alpha} \frac{\text{nucleons}}{\text{m}^2 \text{ s sr GeV}}, \tag{1.1}$$

where E means energy per nucleon and $\alpha = 2.7$ is the differential spectral index of the cosmic ray flux [7]. The equation (1.1) implies energy range from several GeV to beyond 100 TeV. Primary nucleons mainly consist of free protons (79%) and helium nuclei (14.5%) [7].

The secondary flux results from primary particles interacting with gas in the atmosphere. Muons are the products of pion decay and are generally produced at 15 km from the ground [7]. They lose about 2 GeV in passing through the atmosphere due to ionization. The mean energy at sea level is approximately 4 GeV and, as seen in figure 1.1, they are also the most numerous charged particles at the sea level. For very thick objects, the absorption of muons can be used

to radiograph structures of interest.

Using the absorption signal for radiographic measurements is similar in principle to conventional X-ray radiography. This has been implemented for example in scanning the Pyramids of Giza [1] and in probing the internal structure of volcanoes [8].

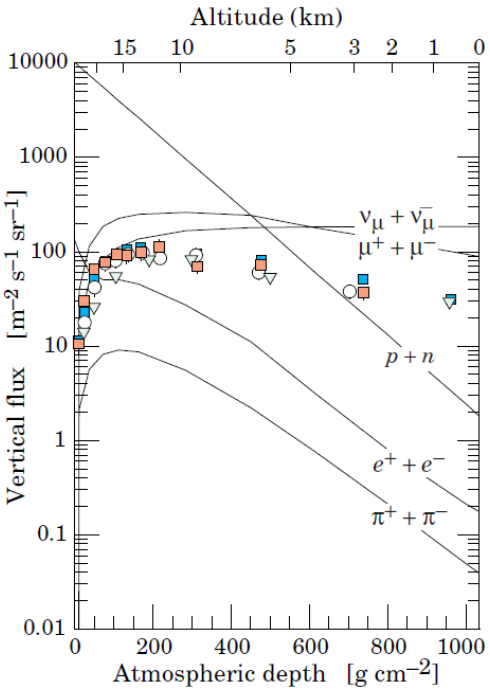

Figure 1.1: Vertical fluxes of cosmic rays in the atmosphere [7]

1.2 Multiple scattering

Recently, alternatives for muon absorption radiography have been developed that utilize multiple scattering. The usefulness of exploiting the deflection angles of cosmic ray muons has been demonstrated for both radiography [2] as well as for tomographic imaging [3] of high-Z materials. Priedhorsky *et al.* have shown that it takes approximately one minute to form useful images using the natural flux ($\frac{10000}{\text{m}^2\text{min}}$ [2, 3, 4]) of cosmic ray muons [3].

Multiple scattering is fundamentally caused by the elastic scattering of a charged particle (e.g. μ^- or e^-) due to the electric field of the atomic nucleus. A particle entering matter will experience several sequential deflections by different nuclei which result in a random walk. Eventually the particle will leave matter at some angle, called the deflection angle, that is different from the incident angle. Each individual particle is scattered at an angle that cannot be exactly predicted, instead, the behavior is probabilistic.

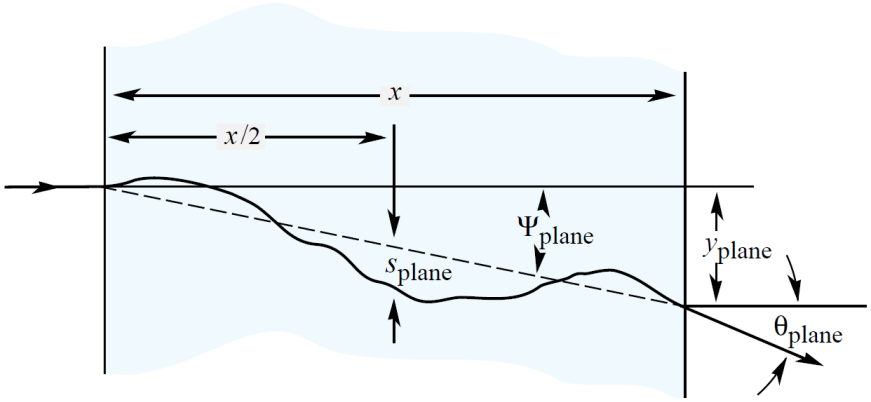

Figure 1.2: Multiple Coulomb scattering [7]

98% of the distribution of deflection angles can be described as Gaussian for many applications, even though there are wings to this distribution [2]. The expression for the Gaussian corresponding to deflection angles is [6, 7]

$$\frac{dN}{d\vartheta_{plane}} = \frac{1}{\sqrt{2\pi}\vartheta_0} e^{-\frac{\vartheta_{plane}^2}{2\vartheta_0^2}}, \tag{1.2}$$

where $\vartheta_0 = \vartheta_{plane}^{rms} = \frac{1}{2}\vartheta_{space}^{rms}$ is the root mean square of the projected angular distribution. This quantity represents the width of the distribution and it is often approximated by

$$\vartheta_0 = \frac{13.6\text{MeV}}{\beta cp} z\sqrt{\frac{x}{X_0}}\left[1 + 0.038\ln\frac{x}{X_0}\right], \tag{1.3}$$

where z is the charge number of the incident particle, p is the particle momentum in MeV, $\beta \cdot c$ is the particle velocity, x is the thickness of the scattering medium and X_0 is referred to as radiation length [7, 9]

$$X_0 = \frac{716.4}{Z(Z+1)\ln\frac{287}{Z}} \quad \frac{\text{g}}{\text{cm}^2}. \tag{1.4}$$

Here Z is the atomic number of the scattering medium. Since the logarithmic term only contributes approximately 10% and $\left|z_\mu\right| = 1$, a further approximation can be used [6]:

$$\vartheta_0 = \frac{14\text{MeV}}{\beta cp}\sqrt{\frac{x}{X_0}}. \tag{1.5}$$

1.3 Muon tomography

From the equations (1.5) and (1.4) it follows that the width of the distribution depends strongly on the atomic number of the material. This dependency, depicted in figure 1.3, can be implemented in the detection of high-Z materials inside an environment of low-Z materials.

A detection system capable of screening such environments (figure 1.4) needs to register the incident muon track as well as the track after scattering. This means that the area to be imaged

needs to have at least one pair of detectors on the opposite sides of the object, so that one group of detectors registers the incident muon and the other group of detectors registers the scattered muon. This screening method is both safe compared to conventional X-ray based techniques and also capable of detecting potential threats in complex cargo scenes in the time scale of minutes [6].

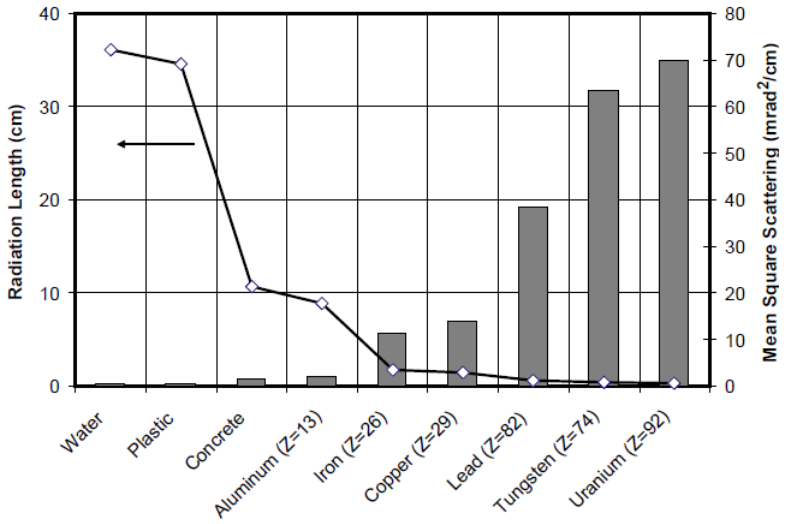

Figure 1.3: The radiation length and the scattering angle depend on the Z of the material. This figure describes 3 GeV muons [4].

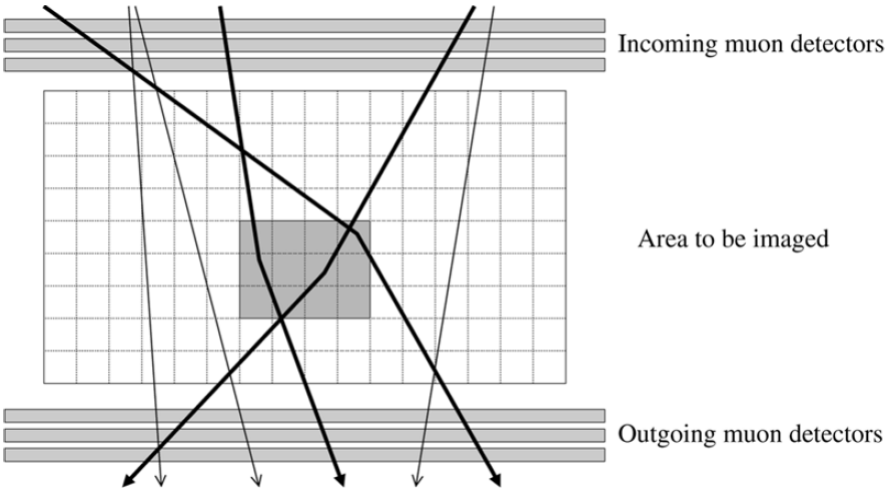

Figure 1.4: The black tracks represent muons penetrating a dense object (gray box) and the gray tracks represent those that scatter through the air. [10].

Chapter 2

Methodology

This chapter gives a brief overview of the simulation software as well as the Monte Carlo methods it implements. More detailed information about Geant4 can be found from the collaboration website[1].

2.1 Monte Carlo methods

Monte Carlo methods are one of the best practical ways to sample random variables that are governed by non-uniform probabilities. The simulation toolkit used in this thesis implements a combination of the rejection algorithm and the method of composition as a means to imitate distributions occurring in physical models.

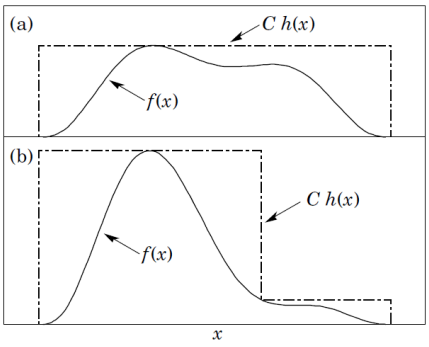

Figure 2.1: An illustration of the rejection sampling method [7]

The rejection sampling method assumes some probability density function $f(x)$ that can be computed. The method also assumes that enough is known about $f(x)$ so that one can enclose the function inside the shape that is a multiple of some constant C of some other distribution $h(x)$ [7]. The distribution $h(x)$ needs to be easily generated, e.g. a uniform distribution. It is worthwhile to note that in the case of Geant4, pseudorandom distributions are provided by the CLHEP [11, 12]. If a randomly chosen point exceeds $f(x)$, the point will be rejected, otherwise it will be accepted. As a result, a set of

[1] `http://geant4.cern.ch`

random numbers will be generated that follow the theoretical distribution $f(x)$. In other words, a simulation or a model of a distribution will be created.

This method can be useful wherever non-uniform probabilities are present. The most relevant example to this thesis is of course multiple scattering. As already described, multiple scattering is a probabilistic process which very closely follows a Gaussian distribution. The way in which this distribution can be simulated is by enclosing the Gaussian distribution inside a uniform distribution, generating random points inside the uniform distribution and rejecting every point that does not belong to the Gaussian. There are many other processes in which rejection sampling is implemented: decay in flight, ionization, dose computation etc.

The method of composition assumes that the desired normalized probability density function $f(x)$ can be decomposed into the sum of several normalized probability density functions f_j:

$$f(x) = \sum_{j=1}^{n} p_j f_j(x), \tag{2.1}$$

where the normalizing constants $\sum_{j=1}^{n} p_j = 1$ and n is the number of terms that $f(x)$ is split into. Suppose, for example, that $f(x)$ can be decomposed into $f(x) = pf_1(x) + (1-p)f_2(x)$. Let us also suppose that we can generate two uniform distributions u_1 and u_2. The algorithm then sets

$$\begin{cases} x = F_1^{-1}(u_2), & \text{if} \quad u_1 < p, \\ x = F_2^{-1}(u_2), & \text{if} \quad u_1 \geq p, \end{cases} \tag{2.2}$$

where F_1^{-1} and F_2^{-1} are the inverse functions of the cumulative distribution functions F_1 and F_2. This method may be used to save computation time.

2.2 Geant4

Geant4 is a computer simulation toolkit designed to track particle motions and interactions. The toolkit is implemented in the C++ programming language and exploits object-oriented principles. Object-oriented design allows for more effective and easily manageable code compared to procedural code. It has been used in the simulations of various scientific fields, for example in nuclear physics, space engineering and accelerator design [13].

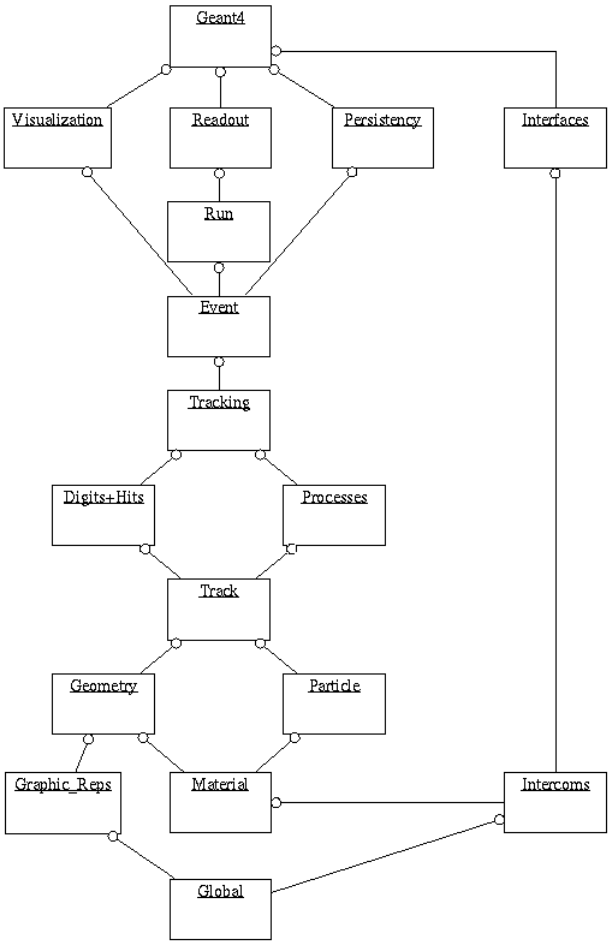

Figure 2.2: A description of the Geant4 class categories [13].

The toolkit consists of classes that are themselves categorized into different class categories, e.g. geometry, interactions, tracking management, visualization etc. These class categories are each individually managed by a work group of the Geant4 international collaboration [13].

Geometry and detection systems are constructed by using two concepts: logical volume and physical volume. The information held by physical volume can be independent of its position in the detector. This information includes material behavior [13]. Physical volume on the other hand places the logical volume in some specific location in space with respect to a mother volume.

All of the basic particle properties, such as mass and charge are described in the `G4ParticleDefinition` class. This class also enables the particle to carry the processes to which it is sensitive. Actual particle properties are described in different extensions of the `G4ParticleDefinition` class. For example muons are described in `G4MuonMinus`. This inheritance can be seen in figure 2.3.

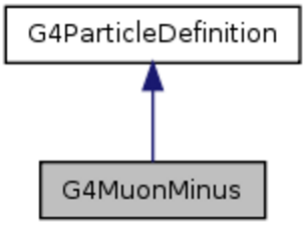

Figure 2.3: Inheritance diagram generated by Doxygen, a tool for generating C++ documentation [14].

Tracking is managed by the `G4TrackingManager` interface and it does not depend on the particle type [13]. Tracking is optimized by the use of voxels, which are created by subdividing the simulation space into volume elements. Tracks, which are represented by objects in C++, are handled by stacks.

2.2.1 Physical processes in Geant4

A process in Geant4 describes a certain initial and a final state. For different physical processes, seven class categories exist in Geant4. These categories are: electromagnetic, hadronic, transportation, decay, optical, photolepton hadron and parametrization. A process is what limits a step. Post step action is provoked after the selection of the process which returns the smallest distance. This algorithm is repeated until the particle is terminated and secondary particles are generated.

The processes most relevant to muon simulations are those responsible for the energy loss of muons and, of course, multiple scattering. Energy loss of muons is computed with a contribution from three different processes: ionization, bremsstrahlung and the production of e^+/e^- pairs. The corresponding classes responsible for these processes are `G4MuIonisation`, `G4MuBrehmsstrahlung` and `G4MuPairProduction`. These are all extensions of the `G4VMuEnergyLossProcess` class. The continuous energy loss is the sum of the different energy loss processes.

Geant4 has several classes dedicated to multiple scattering and it is capable of handling all charged particles [13]. The super class `G4VMultipleScattering` is extended by several classes, including the one which is dedicated to muons: `G4MuMultipleScattering`. The scattering process in Geant4 is described by a model which simulates the scattering of a particle after a step and computes the mean lateral displacement and a correction for the mean path length [13].

Chapter 3

Simulations

3.1 Simulation setup

The simulations were carried out with a very simple geometric setup. The dimensions and shapes were chosen so that they would be similar to a real scenario, but still as simple as possible. The chosen model represents a container and an object to be detected which is placed inside the container.

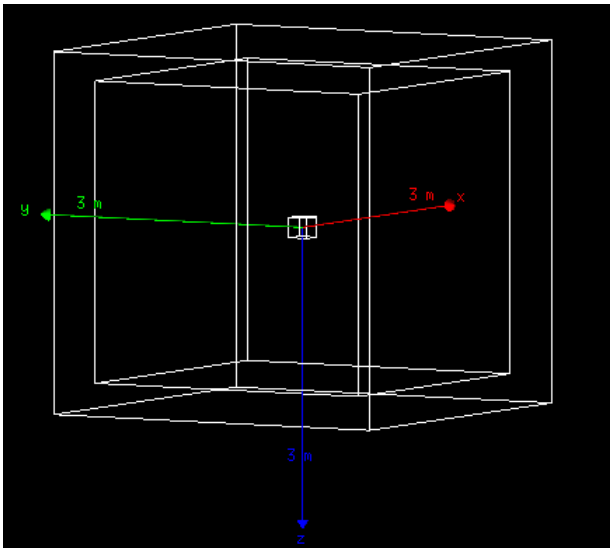

Figure 3.1: A 3 m^3 container with a 10 cm^3 object inside.

The height (z-direction) is set to 3 meters which is similar to standardized container heights (2.9 meters). The x and y directions are for simplicity also defined to be 3 meters, as these dimensions do not have any effect on the simulation results. The size of the world around the container is defined to be 1.2 times the height of the container. The 10 cm^3 object of interest is

placed exactly in the center of the container.

The object of interest is surrounded by air. In Geant4 air can be described by a built-in parameter (`G4_AIR`) which gets its properties from the NIST database. The surrounding material was not changed throughout the process of producing simulation results so that the surrounding environment would be identical for all runs.

As for the object inside the container, various materials were studied. Since multiple scattering in high-Z materials is already a thoroughly studied subject, we decided to focus on simulating multiple scattering in low-Z materials. This is also a very interesting topic to be studied, since there are currently no known ways to detect any low-Z illicit materials inside an environment of some other low-Z material.

The particle gun in this scenario is set to produce a monoenergetic μ^- beam. The energy was set to represent the mean energy of cosmic ray muons at the sea level (4 GeV) so that the results would be comparable to the scattering of real muons. For each material 1000 simulations were run.

3.2 Calculating the scattering angles

Data about the positional information of the penetrating muon is obtained via the `TrackingAction.cc` class (see appendix). This class tracks both the initial position of the incoming particle (x_i, y_i, z_i) as well as the final position of the particle (x_f, y_f, z_f). Output data include positions for x, y and z as well as the length l of the particle track.

To obtain scattering angles θ_j, one has to apply simple rules of trigonometry. For a particle source parallel to the z-axis $\Delta z = z_i - z_f$, where z_i is the initial position and z_f is the final position of the particle. The change in direction on the xy-plane is

$$\Delta s = \sqrt{(\Delta x)^2 + (\Delta y)^2} = \sqrt{(x_i - x_f)^2 + (y_i - y_f)^2}. \tag{3.1}$$

Since the object of interest in our case is placed directly in the center of the container ($\Delta z/2$), the scattering angle θ_j can be found from

$$\tan\theta_j = \frac{\Delta s}{\Delta z/2} \Leftrightarrow \theta_j = \arctan\frac{\Delta s}{\Delta z/2}. \tag{3.2}$$

Finally, to characterize the results of an experiment or a simulation, one could use the arithmetic mean

$$\theta = \frac{1}{n}\sum_{j}^{n}\theta_j. \tag{3.3}$$

Another way to find the scattering angle, which is more similar to the description in chapter 1, is to project the angle to some plane, e.g. the yz-plane and use the root mean square of the Gaussian distribution of all the projected angles. Finding the projected angle is simpler, since only the value of Δx (for projecting on the xz-plane) or Δy (for projecting on the yz-plane) is needed. The projected angle can be found from

$$\theta_{plane} = \arctan\frac{\Delta y}{\Delta z/2}. \tag{3.4}$$

The RMS angle is then

$$\theta_0 = \theta_{plane}^{rms} = \sqrt{\frac{1}{n}\sum_{i=1}^{n}\theta_{plane,i}^2}, \tag{3.5}$$

where n is the number scattering angles found. In the simulations of this thesis, for each material studied, $n = 1000$. This, of course, assumes that no muon goes through a decay process inside the container. Since any of the runs did not result in the decay process, we did not have to take this into account.

Chapter 4

Results and analysis

The simulations were carried out with several materials. Both pure materials (Cu, Pb) as well as compound materials (water, cellulose nitrate) were used. Note that throughout this chapter the simulation screenshots depict the accumulated events of 100 runs, but numerical data, as well as the histograms always describe 1000 runs.

4.1 Results

Simulations were done using a variety of different materials, including one simulation without any object placed inside the container at all. The exact numerical values for the materials are outlined in table 4.1. Each material is described by three different quantities. The first quantity (θ) expresses the deflection angle in milliradians and is found by calculating the arithmetic mean of all the deflection angles according to equations (3.2) and (3.3). The second quantity (θ_0) also describes the deflection angles, but it is found by calculating the root mean square of the projected angles according to equations (3.4) and (3.5). The final column in table 4.1 expresses θ_0 per unit depth of the material through which the muons penetrate.

Material	θ (mean) [mrad]	θ_0 (RMS method) [mrad]	Scattering per unit depth [$\frac{\text{mrad}}{\text{cm}}$]
Air	0.3597	0.2872	0.0009
Water	3.0282	2.6126	0.2613
Nitrocellulose	3.7320	3.0805	0.3081
Cu	17.6905	13.7791	1.3779
Pb	29.8819	24.1617	2.4162

Table 4.1: A comparison of different materials and their respective multiple scattering angles

The results show that the magnitude of multiple scattering is dependent on the value of Z

of the material, as described by literature and as we expected. One can also notice that the two methods of calculation result in slightly different values. Namely the RMS calculation of projected angles tends to produce numerical values that are about 80% of the angles found with the arithmetic mean method. This is not a coincidence, since the exact relationship should be $\theta = \sqrt{\pi/2}\theta_0$ [3].

The simulation results were also visualized with the help of OpenGL[1] and these results can be seen in the figures ahead. Red trajectories depict the passage of muons. Other colors show the traces of non-muon particles (green for gammas, blue for electrons) and enable us to see other physical processes (besides multiple scattering) that are going on inside the system.

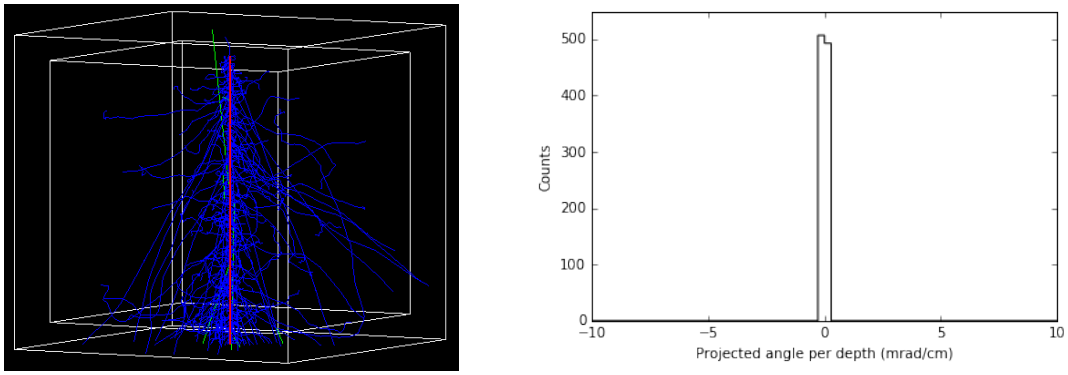

(a) A collection of 100 runs without any objects inside the container.

(b) Distribution of projected angles in air

Figure 4.1: Muons passing through air.

Figure 4.1a depicts the passage of muons through air, i.e. without any object placed inside the container. The blue traces, which represent electrons, depict how the muons induce ionization throughout their passage. It can be seen that almost no other processes besides ionization take place in this collection of runs. Note also that the red beam which represents 100 muons does not diverge almost at all, which shows that the magnitude of multiple scattering is small without the presence of any high-Z materials. This is further illustrated in figure 4.1b which depicts the distribution of scattering angles. The distribution is clearly a sharp peak centered around the vertical axis.

As the value of Z increases, so does the distribution of scattering angles. This can clearly be seen in figures 4.2-4.5. Figure 4.2 depicts the simulations of two composite materials: water and cellulose nitrate. Both of these materials are composed of relatively low Z elements (oxygen, hydrogen, carbon, nitrogen). The accumulated traces produced by 100 runs in figure 4.2 show how each muon is more likely to experience bremsstrahlung compared to the simulations done

[1] https://www.opengl.org/

in air alone. More importantly, the incident muon beam begins to slightly diverge as it penetrates the hidden object.

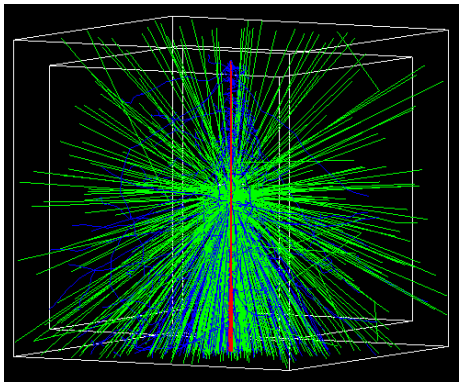

(a) The accumulated events of 100 μ^- in nitrocellulose.

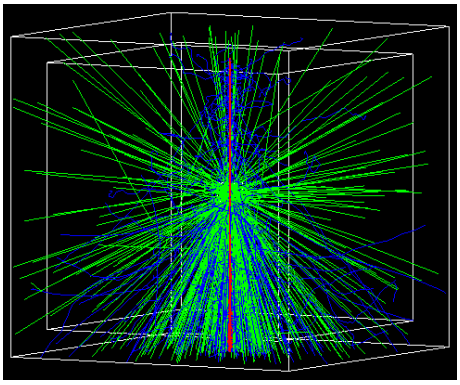

(b) The accumulated events of 100 μ^- in water.

Figure 4.2: A visual comparison of 4 GeV muons scattered from two compound materials.

The same thing can be seen in 4.3 which depicts the distribution of 1000 projected scattering angles for the two composite materials. These distributions are not perfect peaks like the distribution produced by scattering in air. Instead, these distributions are slightly more disperse and therefore the corresponding RMS value of the deflection angle projections is larger as well. Note that the maximum value of the vertical axis is smaller compared to 4.1b.

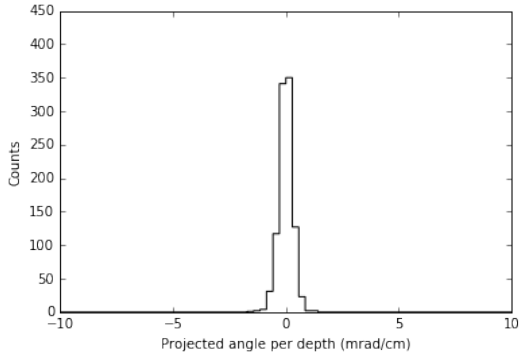

(a) Distribution of projected angles for cellulose nitrate.

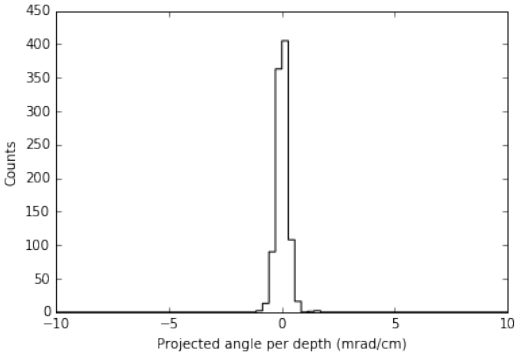

(b) Distribution of projected angles for water.

Figure 4.3

Finally, we studied multiple scattering in two pure materials with an increasing value of Z. The results are depicted in figures 4.4 and 4.5. From 4.4 it can be seen that the incident muon beam diverges a lot more compared to all the previous simulations. The distributions become increasingly wider which means that the likelihood of the projection to deviate away from the center becomes greater if we study higher Z objects.

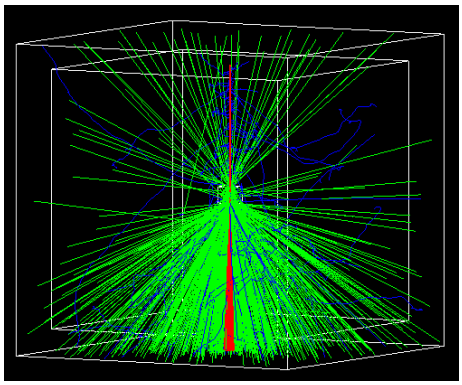

(a) The accumulated events of 100 μ^- in Cu.

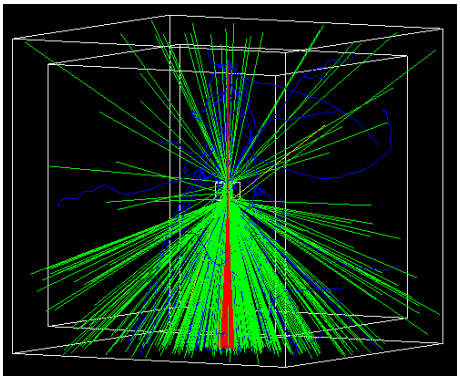

(b) The accumulated events of 100 μ^- in Pb.

Figure 4.4: A visual comparison of 4 GeV muons scattered from two pure materials.

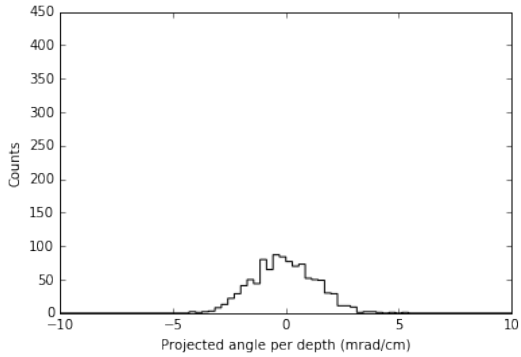

(a) Distribution of projected angles for Cu.

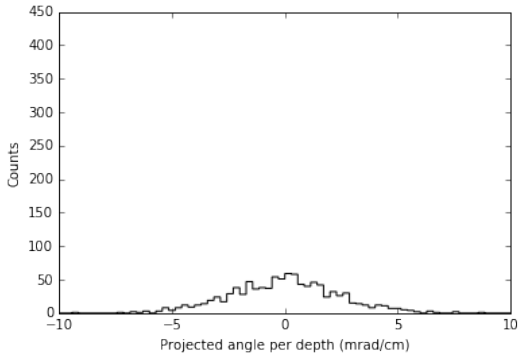

(b) Distribution of projected angles for Pb.

Figure 4.5

4.2 Discussion

The results show that angles produced by the process of multiple scattering change significantly when comparing low-Z and medium-Z materials. For this reason cosmic ray muons can be a powerful tool for identifying medium-Z or high-Z materials in an environment of low-Z materials. This is precisely what can be found from the relevant literature [2, 3, 6, 10]. The numerical values are also similar to those found from literature. For example our value for the RMS deflection angle for water ($\theta_0 \approx 2.6$ mrad) is similar to the angle described by Morris et al. (2008) for 3 GeV muons scattering from a 10 cm thick body of water (2.3 mrad).

Unfortunately, the spatial resolution of modern scintillation detectors limits our capability to detect low-Z materials inside a similar low-Z environment. A realistic scintillator with a spatial resolution of 5 mm x 5 mm would correspond in our experiment to an angular resolution of $\Delta\theta = \arctan\frac{5\text{mm}}{1800\text{mm}} \approx 2.8\text{mrad}$. This means that in real life applications it would not be possible

to see any clear differences between the tomographic images produced by e.g. water ($\theta_0 = 2.6$ mrad) and a low order explosive such as nitrocellulose ($\theta_0 = 3.1$ mrad). A method capable of distinguishing between different low-Z materials inside a low-Z environment would therefore need some additional complementary detection system. One idea is to exploit the attenuation and/or multiple scattering of cosmic ray electrons. This is an area for further investigation.

Our results also show that the method in which an average angle is calculated can make a significant difference in the final results. Table 4.1 shows clearly that by simply finding an arithmetic mean of all the scattering angles, one yields a result that is systematically different from the results found by following the methods outlined in literature. According to table 4.1, the arithmetic mean value is on average about 1.2 times larger than the numerical value found by calculating the RMS of the projected angle distribution. The difference should be kept in mind when designing an experiment or a simulation and interpreting the results, since it might become a source of confusion. It is important to note that although there are different definitions of scattering angles, they all represent the same physical process.

Conclusions

Modern RPM technologies are able to identify only high-Z materials due to greater scattering angles, compared to low-Z materials. This is certainly useful in detecting some important dangerous materials, such as HEU or WGP. Unfortunately, most of the illegal low-Z composite materials (e.g. drugs, explosives) remain undetected by the RPMs. This naturally leads to the question of how a detection system capable of detecting low-Z materials could be constructed and what the main difference would be compared to a system that can only detect high-Z materials.

To answer the question of how well cosmic ray muons could be implemented to identify low-Z materials, a 3 m^3 container and a 10 cm^3 material hidden inside it were modeled. The Monte Carlo simulations showed that in order to detect low-Z materials using cosmic rays, one cannot use the multiple scattering of cosmic rays alone. Instead, additional methods would be necessary. These additional methods could take the form of exploiting cosmic ray electrons or it might also mean using an additional particle source in the design of the detection device.

The next step in this area of research would be to continue studying multiple scattering with other cosmic ray particles and to combine different detection methods as well. In order to produce more realistic simulations, several steps can be taken. These include using a more realistic flux of cosmic ray particles instead of a single monoenergetic beam, designing more complex scenery and simulating the behavior of real detection devices.

Acknowledgements

I would like to thank my advisors Madis Kiisk and Volodymyr Gulik for introducing me to the topic of muon tomography, helping me with the technical details of Geant4 simulations and giving feedback on the progress throughout the year. Thank you for the Geant4 collaboration for not only providing the toolkit, but also the example problems, which helped a lot in designing the setup for the simulations related to this thesis. Finally, I would like to thank my family for all the support and encouragement throughout the years.

Bibliography

[1] Luis W. Alvarez et al. Search for hidden chambers in the pyramids. *Science*, 167:832–839, 1970.

[2] Konstantin N. Borozdin, Gary E. Hogan, Christopher Morris, William C. Priedhorsky, Alexander Saunders, Larry J. Schultz, and Margaret E. Teasdale. Surveillance: Radiographic imaging with cosmic-ray muons. *Nature*, 422(6929):277–277, 2003.

[3] William C. Priedhorsky, Konstantin N. Borozdin, Gary E. Hogan, Christopher Morris, Alexander Saunders, Larry J. Schultz, and Margaret E. Teasdale. Detection of high-z objects using multiple scattering of cosmic ray muons. *Review of Scientific Instruments*, 74(10):4294–4297, 2003.

[4] Larry Joe Schultz, Konstantin N. Borozdin, John J. Gomez, Gary E. Hogan, J. A. McGill, C. L. Morris, W. C. Priedhorsky, A. Saunders, and M. E. Teasdale. Image reconstruction and material Z discrimination via cosmic ray muon radiography. *Nuclear Instruments and Methods in Physics Research Section A: Accelerators, Spectrometers, Detectors and Associated Equipment*, 519(3):687–694, 2004.

[5] Konstantin Borozdin, Thomas Asaki, Rick Chartrand, Mark Galassi, Andrew Greene, Nicolas Hengartner, Gary Hogan, Alexei Klimenko, Christopher Morris, William Priedhorsky, et al. Cosmic-ray muon tomography and its application to the detection of high-Z materials. In *Proceedings of the 46th Annual Meeting, Institute of nuclear Materials Management*, pages 1–8, 2005.

[6] C. L. Morris, C. C. Alexander, J. D. Bacon, K. N. Borozdin, D. J. Clark, R. Chartrand, C. J. Espinoza, A. M. Fraser, M. C. Galassi, J. A. Green, et al. Tomographic imaging with cosmic ray muons. *Science & Global Security*, 16(1–2):37–53, 2008.

[7] C. Patrignani, P. Richardson, O. V. Zenin, R.-Y. Zhu, A. Vogt, S. Pagan Griso, L. Garren, D. E. Groom, M. Karliner, D. M. Asner, et al. Review of particle physics, 2016-2017. *Chin. Phys. C*, 40:100001, 2016.

[8] H. Tanaka, K. Nagamine, N. Kawamura, S. N. Nakamura, K. Ishida, and K. Shimomura. Development of a two-fold segmented detection system for near horizontally cosmic-ray muons to probe the internal structure of a volcano. *Nuclear Instruments and Methods in Physics Research Section A: Accelerators, Spectrometers, Detectors and Associated Equipment*, 507(3):657–669, 2003.

[9] Mukund Gupta. Calculation of radiation length in materials. Technical report, 2010.

[10] Larry J. Schultz, Gary S. Blanpied, Konstantin N. Borozdin, Andrew M. Fraser, Nicolas W. Hengartner, Alexei V. Klimenko, Christopher L. Morris, Chris Orum, and Michael J. Sossong. Statistical reconstruction for cosmic ray muon tomography. *IEEE transactions on Image Processing*, 16(8):1985–1993, 2007.

[11] Mark S Fischler and A Pfeiffer. CLHEP–new developments and directions. Technical report, 2000.

[12] Geant4 Collaboration. Geant4 user's guide for toolkit developers. 2016.

[13] S. Agostinelli, J. Allison, K. Amako, J. Apostolakis, H. Araujo, P. Arce, M. Asai, D. Axen, S. Banerjee, G. Barrand, et al. Geant4—a simulation toolkit. *Nuclear instruments and methods in physics research section A: Accelerators, Spectrometers, Detectors and Associated Equipment*, 506(3):250–303, 2003.

[14] Geant4 Collaboration. Geant4 documentation. `https://www-zeuthen.desy.de/geant4/geant4.9.3.b01/classes.html`, 2009. [Online; accessed 2017-05-13].

Appendix A

Source code

TrackingAction.cc

```
#include <fstream>
using namespace std;
#include "TrackingAction.hh"
#include "G4TrackingManager.hh"
#include "G4Track.hh"
#include "globals.hh"
#include "G4SystemOfUnits.hh"

void TrackingAction::PreUserTrackingAction(const G4Track* aTrack) {

    if ((aTrack->GetTrackID()) == 1) {

        G4cout << "PreTrack position: " << aTrack->GetPosition() << G4endl;
        G4ThreeVector Pos = aTrack->GetPosition();
        G4double xpos = Pos.getX();
        G4double ypos = Pos.getY();
        G4double zpos = Pos.getZ();

        std::ofstream myFile;
        myFile.open("Coordinates.txt", std::ios::app);

        if (myFile.is_open()) {
        myFile << setprecision(5) << std::setw(10) << xpos/m << "\t"
               << setprecision(5) << std::setw(10) << ypos/m << "\t"
               << setprecision(5) << std::setw(10) << zpos/m << "\t";
```

```
        }
        myFile.close();

    };

}

void TrackingAction::PostUserTrackingAction(const G4Track* aTrack) {

    if ((aTrack->GetTrackID()) == 1) {

    G4cout << "PostTrack position: " << aTrack->GetPosition() << G4endl;

    G4ThreeVector Pos = aTrack->GetPosition();
    G4double xpos = Pos.getX();
    G4double ypos = Pos.getY();
    G4double zpos = Pos.getZ();

    std::ofstream myFile;
    myFile.open("Coordinates.txt", std::ios::app);
    if (myFile.is_open()) {
        myFile << setprecision(5) << std::setw(10) << xpos/m << "\t"
               << setprecision(5) << std::setw(10) << ypos/m << "\t"
               << setprecision(5) << std::setw(10) << zpos/m << "\t"
               << setprecision(5) << std::setw(10) << (aTrack->GetTrackLength()
               )/m << G4endl;
    }
    myFile.close();

  };
}
```

Lihtlitsents lõputöö reprodutseerimiseks ja lõputöö üldsusele kättesaadavaks tegemiseks

Mina, Sander Suurpere,

1. annan Tartu Ülikoolile tasuta loa (lihtlitsentsi) enda loodud teose

   Multiple scattering simulations for detection applications,

   mille juhendajad on Volodymyr Gulik, PhD ja Madis Kiisk, PhD,

   (a) reprodutseerimiseks säilitamise ja üldsusele kättesaadavaks tegemise eesmärgil, sealhulgas digitaalarhiivi DSpace-is lisamise eesmärgil kuni autoriõiguse kehtivuse tähtaja lõppemiseni;

   (b) üldsusele kättesaadavaks tegemiseks Tartu Ülikooli veebikeskkonna kaudu, sealhulgas digitaalarhiivi DSpace'i kaudu kuni autoriõiguse kehtivuse tähtaja lõppemiseni.

2. olen teadlik, et punktis 1 nimetatud õigused jäävad alles ka autorile.

3. kinnitan, et lihtlitsentsi andmisega ei rikuta teiste isikute intellektuaalomandi ega isikuandmete kaitse seadusest tulenevaid õigusi.

Tartus, 24. mai 2017. a.